Fuel 371 (2024) 132124

Contents lists available at ScienceDirect

Fuel

journal homepage: www.elsevier.com/locate/fuel

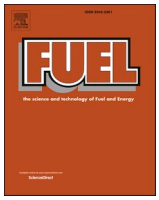

Full Length Article

Computational investigation on spray autoignition of liquid ammonia with dissolved hydrogen in Spray D configuration

Ahmad Hadi Bakir [a], Haiwen Ge [b], Zhili Zhang [a], Peng Zhao [a,*]

[a] Department of Mechanical, Aerospace & Biomedical Engineering, UT Space Institute, University of Tennessee, Knoxville, TN 37388 USA
[b] Zhejiang Lab, Hangzhou, Zhejiang, China

ARTICLE INFO

Keywords:
Liquid ammonia
Spray D
Hydrogen addition
Autoignition
Low carbon fuels

ABSTRACT

Recently, there has been growing interest in ammonia (NH_3) as a carbon-free alternative fuel for ground transportation due to its effectiveness as a hydrogen carrier, and mature infrastructure for production and distribution. Ammonia combustion nevertheless suffers from its slow flame speed, long ignition delay time, and emissions from unburned ammonia, NO_x, and N_2O. As such, future utilization of ammonia might have to involve a dual-fuel strategy, especially with hydrogen, to overcome some of the drawbacks and retain the zero-carbon nature of the system. Our previous work has shown that autoignition of ammonia can be feasible under direct-injection engine conditions with trace amount of gaseous hydrogen addition in the ambient air, which can be potentially introduced from the dedicated exhaust gas recirculation combustion strategy. In the current work, we further investigate autoignition enhancement of liquid ammonia spray with dissolved hydrogen, which can further simplify engine hardware and infrastructure requirement for ammonia-hydrogen dual fuel combustion. Given the trace amount of hydrogen involved, it is assumed that mixture liquid property and spray dynamics does not substantially deviate from pure ammonia, albeit with enhanced chemical reactivity. The solubility of hydrogen is first calculated using the equal fugacity principle. Then, the classical Spray D configuration is adopted for the numerical simulation and validated against existing studies and is extended to the new fuel of ammonia-hydrogen mixture. It is found that the addition of trace amounts of dissolved hydrogen successfully facilitates the ignition of ammonia within reasonable residence time. Furthermore, the results show that varying amount of hydrogen had trivial effect on the ignition timing as the evaporation and mixing are the rate controlling mechanisms for ignition. Compared to hydrogen added via ambient air, fuel dissolved hydrogen shows delayed ignition and flame development. Finally, chemical flux analysis is conducted to provide detailed explanation on the key reaction pathways for ignition and NO_x/N_2O emission.

1. Introduction

Concerns on global warming and climate change have brought attention to the role of fossil fuels in the energy sector. The wide use of fossil fuels has resulted in an increase in greenhouse gases [1], especially carbon dioxide (CO_2), leading to global efforts towards decarbonization [2]. As such, alternative fuels that produce low or zero carbon emissions from their combustion process are becoming increasingly important to achieve carbon neutrality. Most notable are ammonia (NH_3) and hydrogen (H_2), which are being considered as alternatives to fossil fuels due to their zero-carbon nature in the molecule structure. Ammonia has been produced and used extensively in the fertilizer industry thus having a mature production, transport, and storage infrastructure [3]. Additionally, ammonia can be generated from the Haber-Bosch process [4] by synthesizing H_2 and nitrogen (N_2), especially by taking advantage of H_2 generated from renewable energy sources, such as wind, solar, and geothermal energies [5].

Compared to the combustion characteristics of H_2, ammonia suffers from a slow flame speed of 0.07 m/s for stoichiometric fuel–air mixtures at standard temperature and pressure (STP) of 298 K and 1 atm, a long ignition delay time and high latent heat of vaporization. On the other hand, hydrogen has a flame speed of around 2.14 m/s at STP and a substantially shorter ignition delay time. However, compared to hydrogen, ammonia has a much higher boiling point (e.g., 25 °C at 10 bar), as such it has a much higher volumetric energy density compared to hydrogen, where liquid hydrogen exists under cryogenic conditions

* Corresponding author.
E-mail address: pzhao12@utk.edu (P. Zhao).

https://doi.org/10.1016/j.fuel.2024.132124
Received 17 February 2024; Received in revised form 1 June 2024; Accepted 4 June 2024
Available online 8 June 2024

[6]. Thus, the storage, transport and refueling of ammonia as a liquid fuel provides an advantage over hydrogen. However, ammonia as a fuel also suffers from high nitrogen oxides (NO_x) and nitrous oxide (N_2O) formation, due to the nitrogen element in the fuel molecule, and the unburned ammonia-slip. This results in harmful effects on the environment and health. Additionally, the N_2O formed has the Global Warming Potential 300 times of that of CO_2 [7]. Consequently, blends of hydrogen and ammonia are being considered to compromise the drawbacks of the poor combustion characteristics of ammonia and the challenging transportation and fueling options of hydrogen.

Ammonia-hydrogen dual-fuel studies have been conducted for ammonia being the main fuel to make use of its storage and transportation capabilities, while hydrogen being added to improve its combustion performance. Chen et al. [8] investigated the effects of hydrogen blending with ammonia on the ignition delay times in a shock tube. This study utilized the fuel blends of 100 % NH_3, 95 % NH_3/5% H_2, 70 %NH_3/30 % H_2, and 30 % NH_3/70 % H_2. The results demonstrated a nonlinear decrease in ignition delay times with an increase in hydrogen blending ratio. This enhancement can also be observed in relevant engine configurations. Wiseman et al. [9] investigated the blow-out behavior of turbulent premixed ammonia/hydrogen/nitrogen-air and methane-air flames under gas turbine relevant conditions. The fuel ratio selected is 40 % NH_3/45 % H_2/15 % N_2 by volume. The results demonstrate that the addition of hydrogen to the fuel results in an improved heat release rate and fuel consumption rate and suggests that the diffusion of hydrogen is the main cause to enhance the reactivity of the mixture thus improving the combustion characteristics. Dinesh et al. [10] conducted an experimental study on the ammonia and hydrogen blends with five hydrogen energy fractions, 5 %, 9 %, 13 %, 17 %, and 21 %, in a port fueled spark ignition (SI) engine using a range of compression ratios and engine speeds. It was found that hydrogen addition improved the performance of ammonia in a SI configuration while reducing volumetric efficiency. However, increase in compression ratio is shown to increase volumetric efficiency, thus creating an optimization requirement. Furthermore, the NO_x emissions have been shown to increase with H_2 addition as the temperature in the cylinder increases. Bakir et al. [11] numerically investigated ammonia and hydrogen blends ranging from 100 % ammonia mole fraction to 100 % hydrogen mole fraction in increments of 5 % mole fraction under different intake pressure and temperature in a homogeneous charge compression ignition (HCCI). It is found that the crank angle corresponding to 50 % of the heat released (CA50) is more sensitive to the intake temperature rather than pressure. Furthermore, increase in hydrogen concentration, resulted in a lower required intake temperature to achieve a CA50 near top dead center. For diesel engines, the low reactivity of ammonia poses a challenge in its feasibility requiring impractical high compression ratios [12]. As such, studies have been conducted with pilot fuel injection to increase the reactivity of the mixture. Nadimi et al. [13] experimentally investigated ammonia/diesel dual-fuel compression ignition engine in terms of combustion and emissions and the effect ammonia addition has on them while varying the ammonia energy fraction from 0 to approximately 84 %. The results show that indicated thermal efficiency increases with the replacement of diesel with ammonia while the combustion phasing and duration both reduced. Moreover, as ammonia concentration increases, carbon emissions decreased while NO_x and N_2O increased.

However, the direct injection of ammonia in compression engines poses challenges thus methods of promoting ignition in engine relevant conditions are investigated. One such promotion can be achieved through an active pre-chamber ignition system which creates a turbulent jet flame and enhances ignition and combustion in the main chamber. Liu et al. [14] numerically investigated a prechamber's role in improving the efficiency of an ammonia fueled heavy duty engine by optimizing spark timing, prechamber nozzle diameter, and hydrogen energy fraction. The results showed that increasing hydrogen energy fraction from 0.5 to 2 % resulted in an advanced combustion phasing while reducing indicated thermal efficiency due to increased wall heat transfer. Liu et al. [15] experimentally investigated an ammonia fueled engine with a reactivity-controlled turbulent jet ignition system. It is found that improved combustion performance is achieved by increasing the concentration of premixed hydrogen-air in the prechamber and thus increasing the reactivity. However, using ammonia-air premixed mixture in the prechamber resulted in a lower combustion stability as it results in a weaker turbulent jet from the prechamber. Furthermore, despite the narrow flammability range for ammonia, the use of the prechamber showed an improved combustion stability for lean mixtures with an air–fuel ratio of 1.4 resulting in optimized fuel consumption. Huo et al. [16] numerically investigated an H_2 fueled active prechamber in an ammonia/hydrogen port fuel injection engine under lean conditions. They investigated a range of hydrogen energy fraction from 10 to 40 % and an equivalence ratio of 0.4 to 0.6 in the main chamber while maintaining an equivalence ratio of 0.74 in the prechamber. The study demonstrated that a lean H_2 fueled prechamber can operate the main chamber in leaner conditions, which nevertheless needs further optimization. For equivalence ratio of 0.4, higher unburned NH_3 and higher N_2O are observed. On the other hand, NO_x emissions are reduced due to reduced temperatures. The results show that increasing hydrogen energy fraction in the main chamber results in a more reactive mixture, which, however, increases NO_x concentrations.

Recently, the enhancement of ammonia through the use of hydrogen added to the ambient air to facilitate the ignition of ammonia spray has been investigated numerically under engine relevant conditions [17]. The addition of hydrogen can be conducted by dedicated exhaust gas recirculation, which requires one cylinder to run a rich mixture of ammonia to generate additional H_2 that can be recirculated back to each cylinder, or onboard thermal cracking which requires a catalyst to initiate the NH_3 decomposition into H_2 and N_2. The results demonstrated that trace amounts of hydrogen, from 0.043 % to 1.4 % mole fraction in the ambient air, are enough to enhance ignition of ammonia through the production of OH radicals. Another method of introducing H_2 to facilitate ignition is by dissolving H_2 gas into the liquid NH_3 thus creating a fuel blend. By doing so, the fuel will have an increased reactivity through hydrogen while maintaining its liquid form and reduce the cost of retrofitting the current combustion systems. Compared to other dual fuel strategies, such as the port fuel injection of a premixed gaseous fuel blend of ammonia and hydrogen or the injection of liquid ammonia in a hydrogen/air ambient, the current method allows for a direct injection of the liquid fuel blend in compression ignition engines with a single injector. The fuel blend in this case will not be mixed with air in the fuel tank and injection system until it is injected in the combustion chamber. As such, pre-ignition of hydrogen can be avoided. The current work evaluates the performance of a new liquid fuel with trace amount of hydrogen dissolved in ammonia and identifies the role of hydrogen addition on its ignition characteristics in the classical Spray D configuration [18]. This approach is further compared to our previous study with hydrogen addition supplied from the ambient gas. Finally, evaluation of key chemical pathways and emission formation is investigated.

2. Methodology

2.1. Numerical models

In this work, the commercial software CONVERGE 3.1 [19] is used to simulate ammonia spray combustion in the Spray D configuration. The models selected for this study are as follows: the Redlich-Kwong equation of state [20] is used to describe the gas and liquid phase fluids. The Mixture-averaged species transport is used to calculate a diffusion coefficient for each species. Turbulence is modeled through the Reynolds-Averaged Navier-Stokes [21] model using the Renormalization Group k-ε [22] that accounts for the different length scales of motion that contribute to turbulent diffusion. Fuel injection is modeled through the BLOB injection model [23]. As the liquid is injected, its breakup and

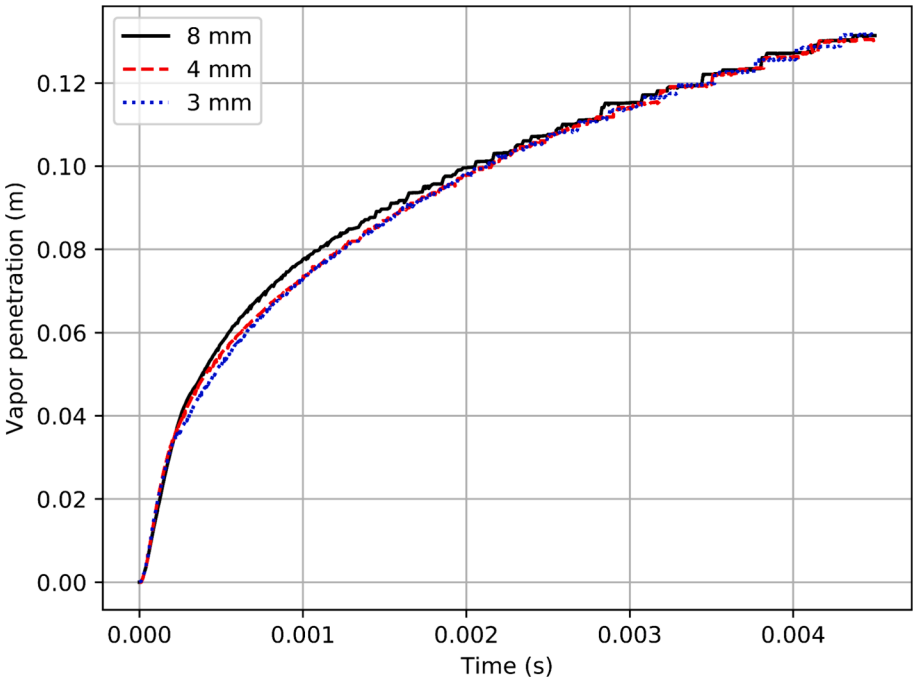

Fig. 1. Vapor penetration of ammonia spray comparing different base mesh sizes.

atomization are modeled through the Kelvin-Helmholtz Rayleigh-Taylor models [24] in addition to the O'Rourke turbulent dispersion model [25]. Furthermore, droplet interactions are modeled through the No-Time-Counter collision model [26] while the drag effects are modeled through the dynamic drop drag model. Considering droplet evaporation, the process is modeled through the Frossling model [25]. The ammonia spray experiments show a high tendency of ammonia to flash boiling [27], and consequently the flash boiling model in Price et al. [28] is used. The SAGE chemistry solver [29] is adopted to model the detailed reactions in the combustion process. In order to investigate the kinetics of ignition and NO_x formation, the mole fractions and thermodynamic condition are extracted from points of interest and inserted into CANTERA [30]. By initializing the mole fractions and thermodynamic conditions into CANTERA, the ReactionPathDiagram class can be used to generate the reaction pathways.

Spray D [18] is an experimental configuration using a one nozzle injector with a diameter of 0.19 mm. The fuel, n-dodecane, is injected into a constant volume chamber at 900 K and 60 bars. The fuel is injected for 4.5 ms with an injection pressure of 1500 bars at a temperature of 363 K. For the ammonia case, liquid ammonia is injected at a temperature of 298 K in order to lessen the effects of flash boiling. Furthermore, the injection pressure is maintained at 1500 bars into the combustion chamber at 1300 K and 60 bars. The ammonia reactive case uses the Otomo et al. kinetic mechanism [31] to model the reactions that has been validated against experimental laminar flame speed, NO_x formation [32] and ignition delay times for ammonia and hydrogen blends [31].

2.2. Mesh

To determine grid independence, a simulation using the Spray D configuration with ammonia as the fuel is conducted. Three base mesh sizes are used, 8 mm, 4 mm, and 3 mm, with a level 5 embedding Adaptive Mesh Refinement (AMR) resolving the temperature and

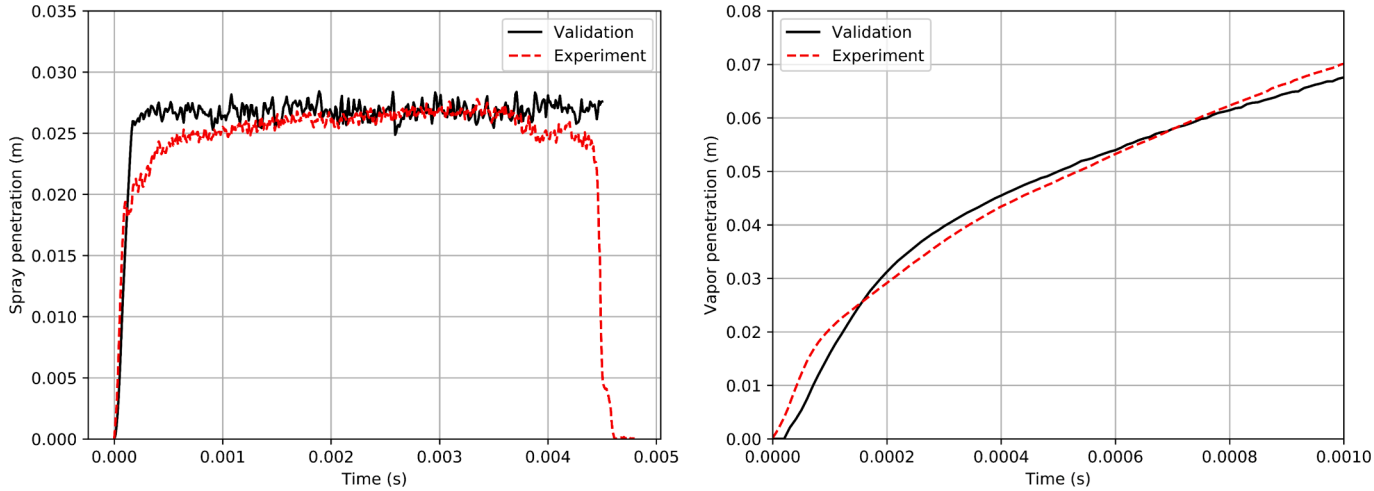

Fig. 2. Comparison of numerical results with experimental data. Liquid penetration on the left and vapor penetration on the right. Experimental data taken from [33] experiment ABKLDDLASRDE.

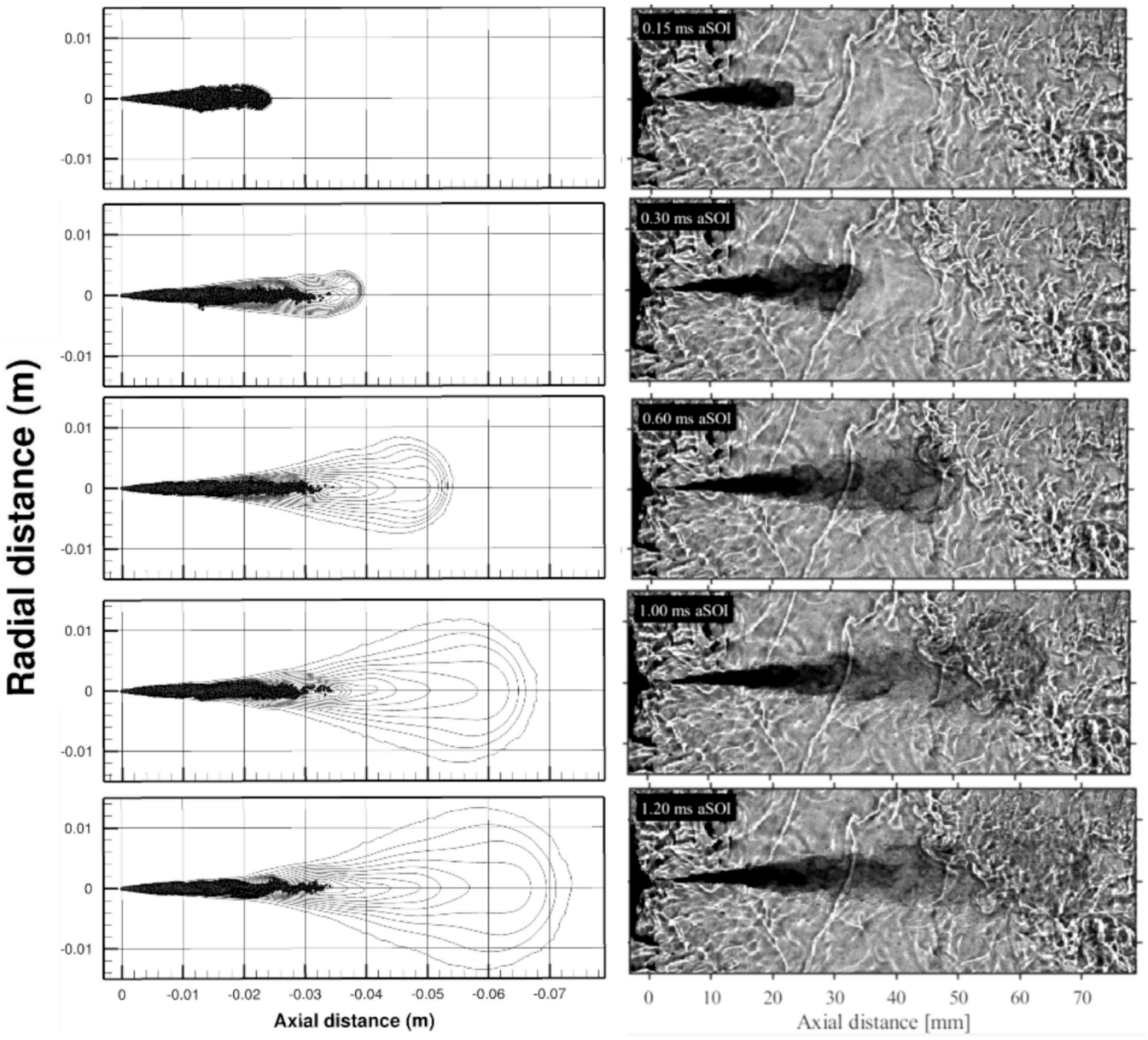

Fig. 3. Spray morphology comparison using n-dodecane mass fraction. Experimental data taken from [33] experiment ABKLDDLASRDE.

velocity gradients in addition to level 5 fixed embedding near the nozzle to resolve the high velocity changes due to injection thus having a minimum mesh size of 0.25 mm, 0.125 mm, 0.09375 mm. Fig. 1 shows the grid independence study conducted for this work by comparing the vapor penetration using different base mesh sizes. It is shown that further refinement of the base mesh size provides negligible differences. As such, the base mesh size for this study is selected to be 4 mm.

2.3. Validation

To gain confidence in the selected models, a validation is conducted using the Spray D experimental results from injecting n-dodecane fuel into a constant volume reactor [33]. The fuel at a temperature of 363 K is being injected into a domain with an ambient temperature, pressure, and composition of 900 K, 60 bar, and 89.71 % N_2, 6.52 % CO_2, and 3.77 % H_2O, respectively. The injection pressure is 1500 bars with a duration of 4.5 ms. The target validation data are the spray penetration, vapor penetration, and spray morphology taken from [33] experiment ABKLDDLASRDE.

Fig. 2 shows the validation results against experimental data using the liquid penetration on the left and vapor penetration on the right. In the simulation case, based on the Engine Combustion Network (ECN) modelling standards [34], the liquid penetration distance is defined as the liquid penetration fraction of 0.99 while the vapor penetration distance is defined by the maximum distance where the fuel vapor mass fraction is 0.001. It can be observed from the liquid penetration that the numerical model shows reasonable overall agreement with the experimental data except for an overprediction at the beginning of injection. The vapor penetration results show a similar trend with a slight underprediction at the beginning of injection. In spray modeling, both penetration and morphology are necessary to provide satisfactory validation. As such, a comparison of spray morphology evolution at selected instants using n-dodecane mass fraction is shown in Fig. 3. As shown, the numerical results demonstrate reasonable agreement with experimental data [33]. Thus, the results give confidence to continue with the ammonia spray cases.

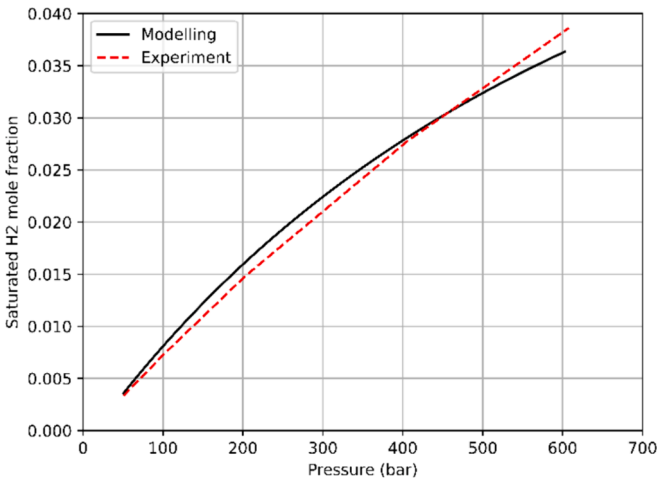

Fig. 4. Comparison of hydrogen solubility in ammonia modeling using PE2000 software against experimental data taken from [41].

2.4. Hydrogen solubility

To determine the amount of hydrogen to be dissolved and the modeling potential of the software, the maximum concentration of hydrogen that can be dissolved in liquid ammonia at a given temperature and pressure (i.e., the solubility of hydrogen in ammonia) needs to be calculated. Solubility is modeled using the Phase Equilibria 2000 (PE2000) software [35] that has been used extensively to calculate solubilities of different mixtures [36 37 38 39]. The solubility of the mixture is calculated using the Redlich-Kwong equation of state [20] based on the fugacity principle where the fugacity coefficients for the vapor and liquid phases are equal at equilibrium. For binary mixtures, a mixing rule needs to be included to account for both components. As such, the Adachi-Sugie mixing rule [40], which has been used in [36] and [37], is used for this work.

Fig. 4 shows a comparison of the numerical modeling against experimental data of the mole fraction of soluble hydrogen in liquid ammonia over a wide range of pressure at 298 K taken from the work of Weibe et al. [41]. As shown, the modeled saturated H_2 mole fraction at different pressures shows good agreement with the experimental data and follows the trend of increase in solubility with pressure.

These results demonstrate the upper limit of dissolved hydrogen in liquid ammonia. At this limit, the mixture will be unstable due to the tendency of hydrogen to separate from the solution as pressure changes. Thus, this work will include an amount of hydrogen significantly less than the solubility to mitigate the mentioned instability. For a 60 bars domain, the limit is the saturated H_2 mole fraction 0.0045. It is expected that as the amount of hydrogen dissolved is in trace amounts, its effect on the liquid properties and spray dynamics become negligible. To satisfy these requirements, an amount of 0.085 %, 0.01 %, and 0.005 % mole fraction of hydrogen is added to the liquid ammonia.

Cases utilizing pure ammonia and ammonia hydrogen addition is modeled to demonstrate the insignificant effect the amount of change the added hydrogen has on ammonia. Fig. 5 shows the vapor penetration comparison. As shown, the vapor penetration shows no notable change in both cases. Fig. 6 shows the radial distribution of NH_3 mole fraction at 25 mm away from the injector at different instances with and without hydrogen addition. As shown, the distribution shows similar results in both cases when comparing the results from the pure ammonia to the dissolved hydrogen addition with and without the chemical source terms. Thus, this setup provides confidence in the model setup while justifying the minimal changes in ammonia spray with trace hydrogen addition.

3. Results and discussion

3.1. Autoignition of pure ammonia

Ammonia is considered a low reactivity fuel with a high ignition temperature, long ignition delay times, and slow flame speed. Additionally, in a spray configuration, ammonia also suffers from charge-cooling effects and flame extinction [17] due to the high latent heat of vaporization [42]. These drawbacks are evident in a pure ammonia injection case. In this case, liquid ammonia at 298 K is injected into a chamber at 1300 K and 60 bars at the start of the simulation for 4.5 ms using the Spray D configuration. Fig. 7 shows the evolution of the temperature contour for the pure ammonia spray. The results show no

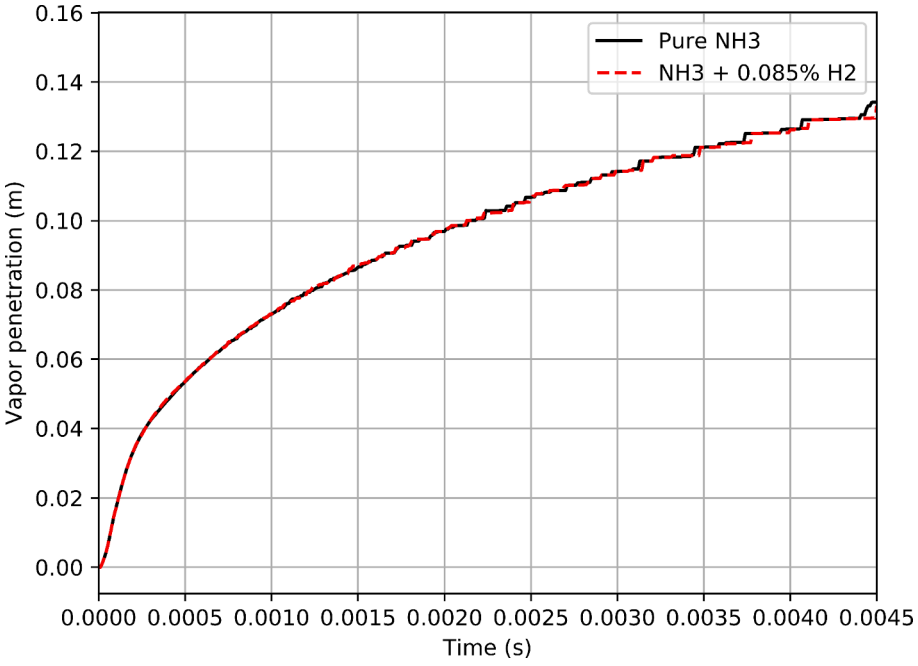

Fig. 5. Comparing vapor penetration of case with pure ammonia and case with 0.085 % dissolved H_2 added to ammonia.

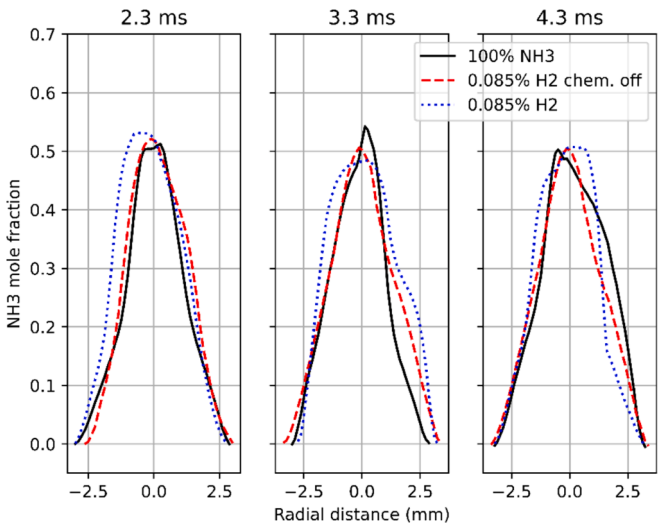

Fig. 6. Comparison of radial distribution of NH_3 mole fraction 25 mm away from the injector between pure ammonia case and 0.085 % mole fraction H_2 dissolved in ammonia with and without the chemical source term used.

increase in temperature indicating no ignition occurring despite being at elevated thermodynamic conditions. These results demonstrate the challenges ammonia has for direct injection applications. As such, increasing the reactivity of ammonia needs to be considered to facilitate ammonia ignition. In this work, hydrogen addition as a dissolved gas in liquid ammonia will be numerically investigated as a method to initiate ignition.

3.2. Ignition process with trace amount of dissolved hydrogen

Fig. 8 shows the evolution of the maximum temperature with time for pure ammonia and fuel blends including 0.085 %, 0.01 %, and 0.005 % dissolved H_2 mole fraction. As the fuel is injected, maximum temperature remains steady the chemical reactions release heat post the evaporation and mixing processes. The maximum temperature is shown to be near 1750 K which is achieved after the end of injection then is followed by a decrease in maximum temperature. Furthermore, the different mole fractions of dissolved H_2 result in similar combustion evolution with time. This is a result of the similarity in evaporation and mixing time scales of the three cases, suggesting that the controlling step for ignition is the dissolved hydrogen, while the combustion evolution after the ignition is mainly depended on the spray dynamics and mixing. This is controlled by the thermophysical properties of primarily liquid ammonia, rather than changes in chemical reactivity with varying amount of hydrogen addition. The higher reactivity of hydrogen compared to ammonia results in its immediate local oxidation, which is largely similar for all three cases regardless of the amount of hydrogen. Thus, the new fuel blend – liquid ammonia with trace amount of dissolved H_2 – provides good flexibility of fuel preparation, and exhibits substantially enhanced chemical reactivity, which is meanwhile insensitive to hydrogen blending ratio due to dominant effects by spray dynamics and subsequent evaporation and mixing of liquid ammonia. To understand the detailed ignition process and the development of the flame, the temperature and equivalence ratio contours of the 0.085 % case are examined.

The decrease in maximum temperature can be explained by the insufficient fuel injection and the low reactivity of ammonia. Despite the oxidation occurring, the heat release and the flame propagation occur slowly thus requiring an extension of the injection duration to allow for the flame to develop and reach its maximum temperature. Furthermore, around 45.9 mg of NH_3 is injected into the domain. Post injection, at 10 ms, around 0.0162 mg of NH_3 is left. Despite most of the fuel being consumed, the flame requires more fuel to be injected to be fully developed and sustained. This is shown in Fig. 9 where the evolution of the local equivalence ratio contour with time is plotted for the case with 0.085 % mole fraction of dissolved H_2.

In Fig. 9, it is observed that once the injection ends the equivalence ratio continues to reduce until the fuel is burned or diffuses in the domain as the air concentration is much higher. This can be further

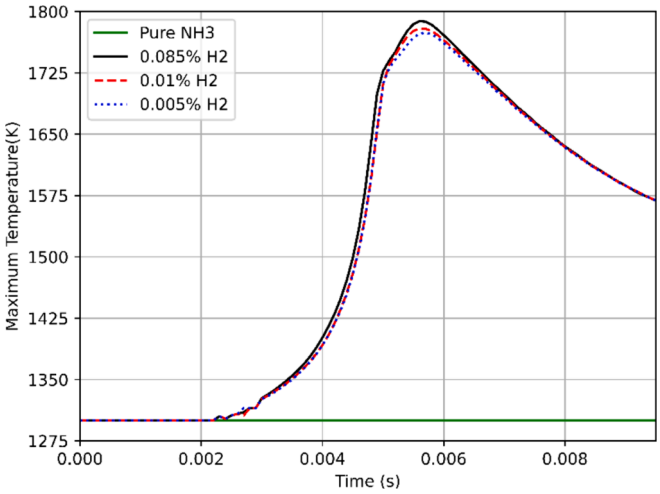

Fig. 8. Evolution of maximum temperature with time for pure ammonia and ammonia with 0.085 %, 0.01 %, and 0.005 % mole fraction dissolved H_2.

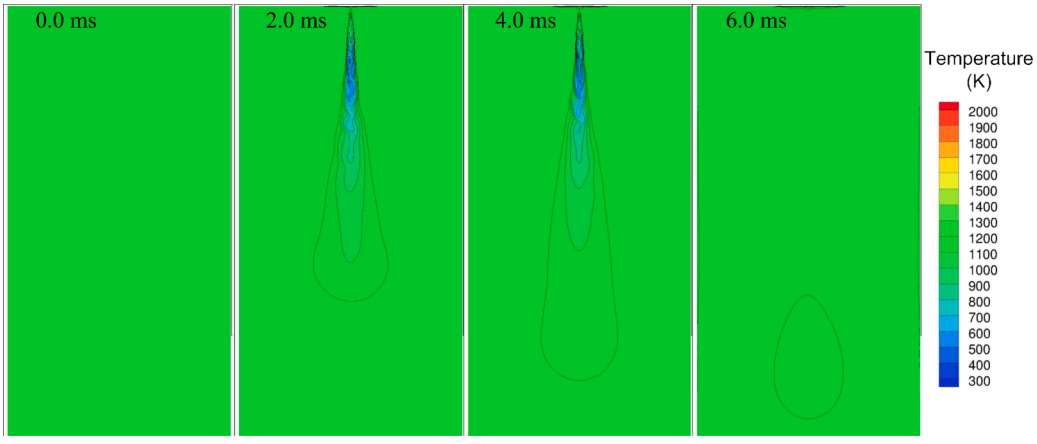

Fig. 7. Temperature contour of pure ammonia spray.

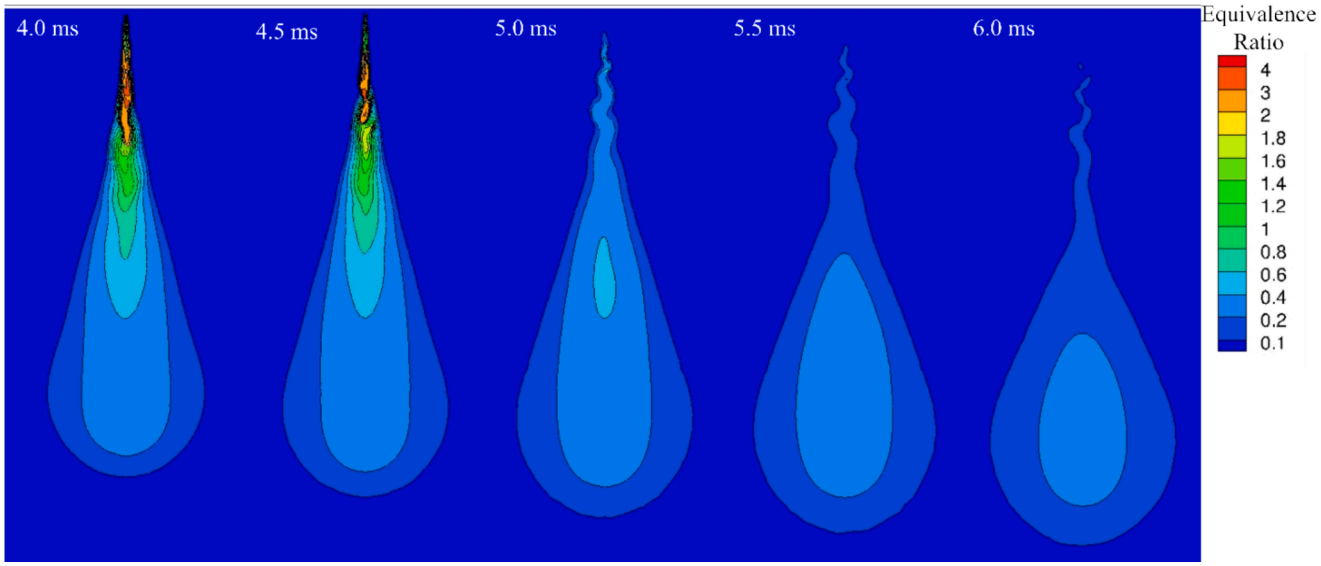

Fig. 9. Local equivalence ratio contour evolution with time for 0.085 % H_2 mole fraction dissolved in liquid ammonia with 4.5 ms injection duration.

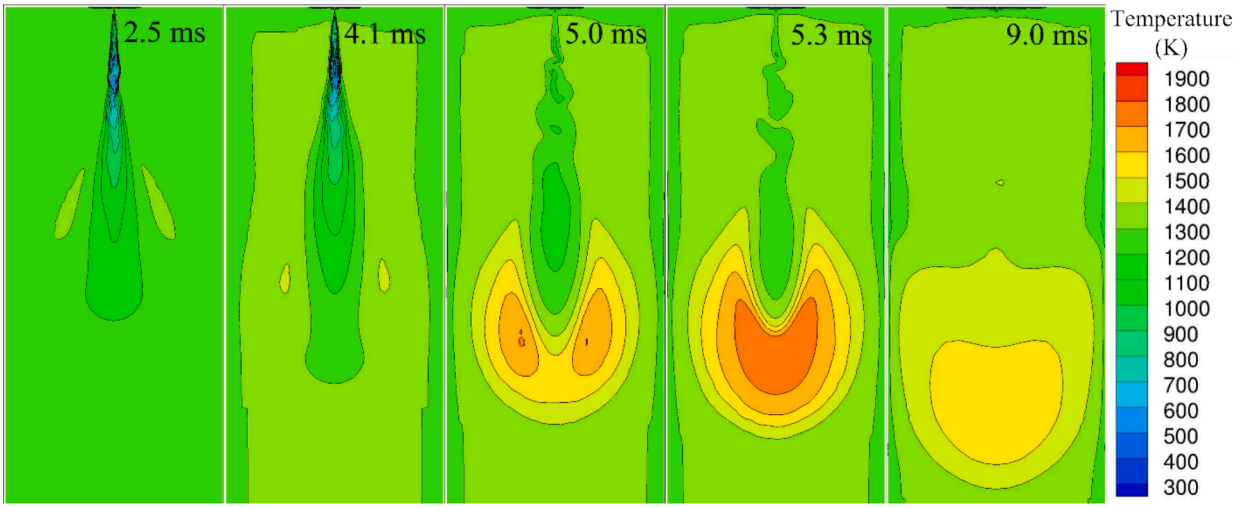

Fig. 10. Temperature contour showing ignition process of ammonia with 0.085 % H_2 addition.

discussed through the number of nitrogen–hydrogen bonds. Starting with a total ammonia mass of 45.9 mg, the leftover mass is 0.0162 mg. NH_2 has two bonds with a leftover mass of 1.57e-4 mg, and NH, which has one bond, is left with 8.34e-8 mg. Thus, by comparing the mols of the left-over bonds with what was injected into the domain, 99.89 % of the bonds are broken into from the NH_i paths. It is important to note that in this case the global fuel to air ratio is 0.00225, which is relatively low. However, this constant volume direct injection configuration provides insights into the spray dynamics and ignition process thus requiring increased injection duration to study a fully developed flame.

Fig. 10 shows the temperature contour evolution of the spray with time for the case with 0.085 % mole fraction dissolved H_2. It is observed that the initial increase in temperature begins on the side of the spray at 2.5 ms. As the temperature continues to increase, ignition kernels are formed on the side of the spray similar to the previous study with hydrogen introduction in the ambient gas [17]. The ignition kernels continue to grow and develop a flame that propagates towards the tip of the spray first then towards the injector. The flame development is shown to begin past the end of injection at 4.5 ms. As such, the flame is not sustained when the injection ends causing the flame to not completely develop. However, this case can provide important insights

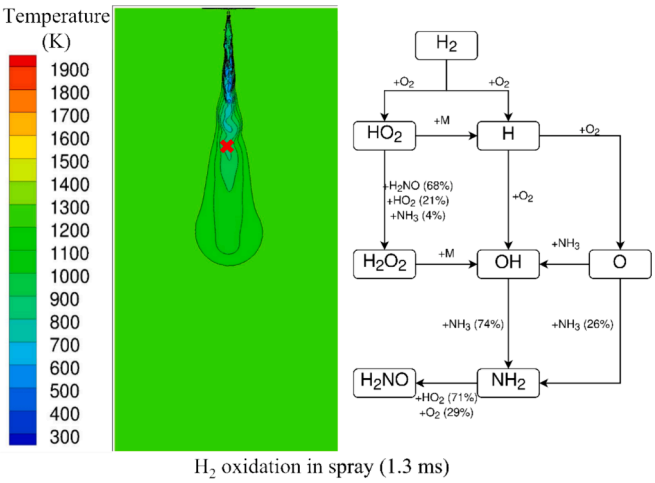

Fig. 11. Chemical kinetic pathway at 1.3 ms for H_2 oxidation.

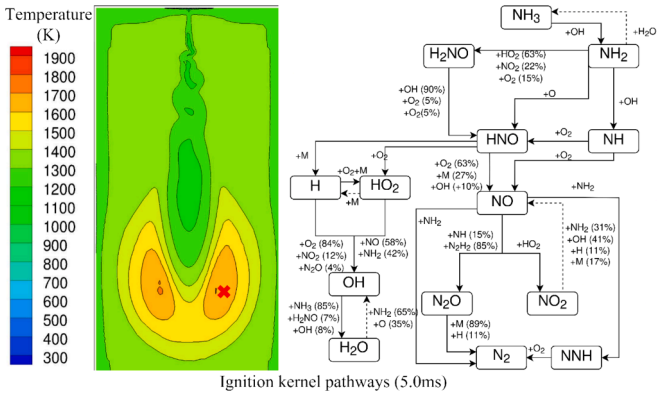

Fig. 12. Chemical kinetics pathway for NH_3 oxidation in the ignition kernels at 5.0 ms.

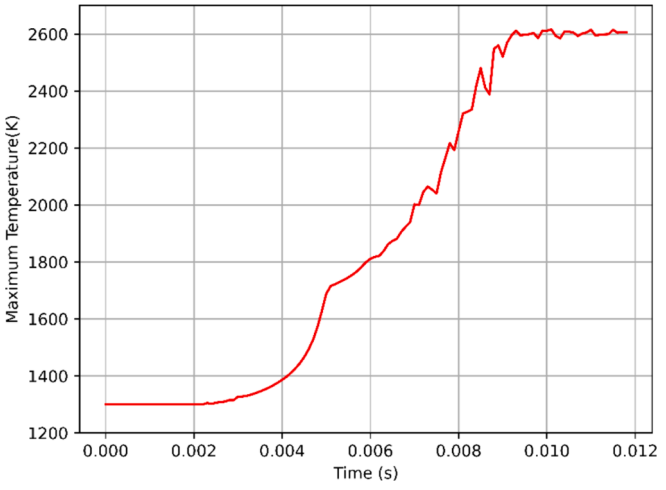

Fig. 13. Maximum temperature evolution with time for 0.085 % mole fraction of dissolved H_2 in liquid ammonia with an injection duration of 12 ms.

into the chemical kinetics of this ignition process. Mole fractions and the thermodynamic state at two separate locations are extracted and input into Cantera [30] to create chemical kinetic pathways diagrams.

Fig. 11 shows the temperature contour plot of the spray at 1.3 ms (left) during the oxidation of the H_2 and radical formation before ignition. The gaseous compositions at the indicated position by a cross are extracted for reaction flux analysis with a thermodynamic condition of 850 K and 60.5 bars. The H_2 oxidation pathways diagram (right) shows H_2 reacts with O_2 to form HO_2 and H radicals. HO_2 further reacts with the third body + M to form more H radicals. The pool of H radicals generated from this process reacts with O_2 to form OH and O radicals. The formed radicals are directly responsible for the oxidation of NH_3 where 26 % of the NH_3 react with O to form OH and NH_2, while 74 % of NH_3 react with OH to form NH_2. Then, NH_2 further forms H_2NO through its reaction with HO_2 and O_2. The resulting H_2NO reacts with HO_2 to form H_2O_2 that reacts with a third body to form more OH radicals. Thus, it feeds into the further oxidation of NH_3.

Fig. 12 shows the temperature contour (left) at 5 ms. The investigated point is inside the ignition kernel with the thermodynamic condition of 1690 K and 62.4 bars. The reaction flux analysis (right) at the ignition kernels follows the consumption of ammonia and ignition. In the ignition kernel, NH_3 continues to oxidize through its reaction with OH. The NH_2 formed further reacts with OH to form NH and its subsequent radicals thus promoting the ignition from the chain reactions. As shown, the radicals formed from the oxidation of H_2 are vital for the oxidation of NH_3. The OH radical plays a vital role in the radical formation throughout the pathways.

3.3. Developed flame

To allow for the formation of a developed quasi-steady ammonia spray flame, the injection duration is extended to 12 ms while maintaining the injection pressure of 1500 bars by increasing the injected fuel mass from 45.9 mg to 122.35 mg thus sustaining the flame with the continued fuel supply.

Fig. 13 shows the evolution of the maximum temperature with time for the extended injection case. As shown, the ignition profile in terms of the maximum temperature is shown to be the same as Fig. 8. However, after 4.5 ms the flame is sustained through the continuous injection of the fuel blend thus allowing it to develop and propagate until it engulfs the spray. Furthermore, as the injection continues until 9 ms, it begins to reach a quasi-steady state of flame temperature. This can also be observed from the temperature contour profile of the spray.

Fig. 14 shows the temperature contour evolution with time for the developed flame case. As shown, the start of the ignition process is similar to the results in Fig. 10. However, the extended injection duration provides sufficient ammonia and time for the flame to develop. Ignition kernels are formed near the tip of the spray on the sides. Once a flame is formed, it propagates from the tip of the spray towards the injector thus engulfing the entire spray. The structure of the flame is as

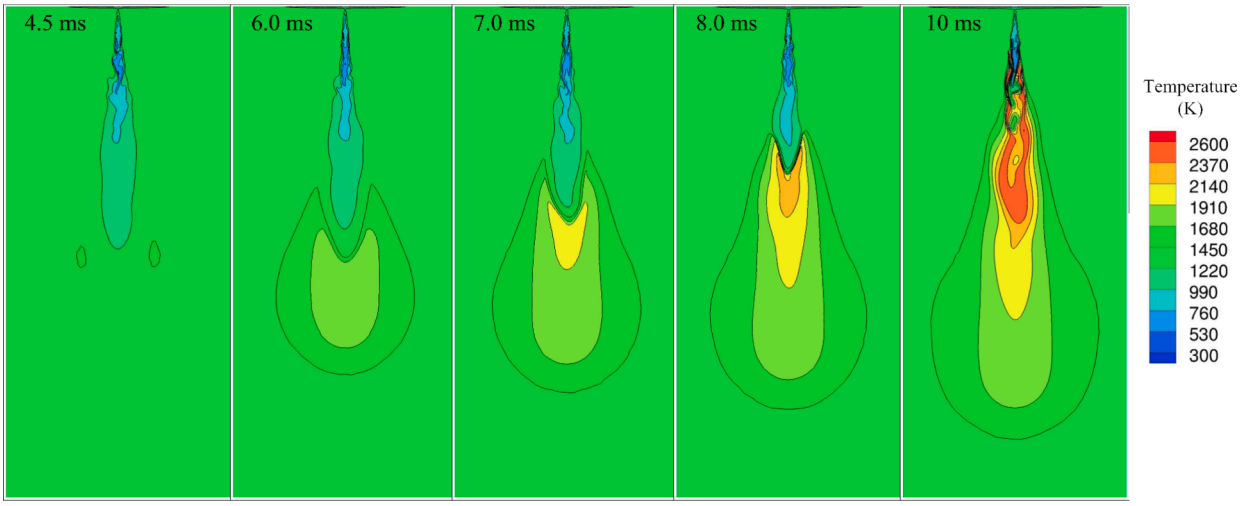

Fig. 14. Temperature contour with extended fuel injection forming the developed flame.

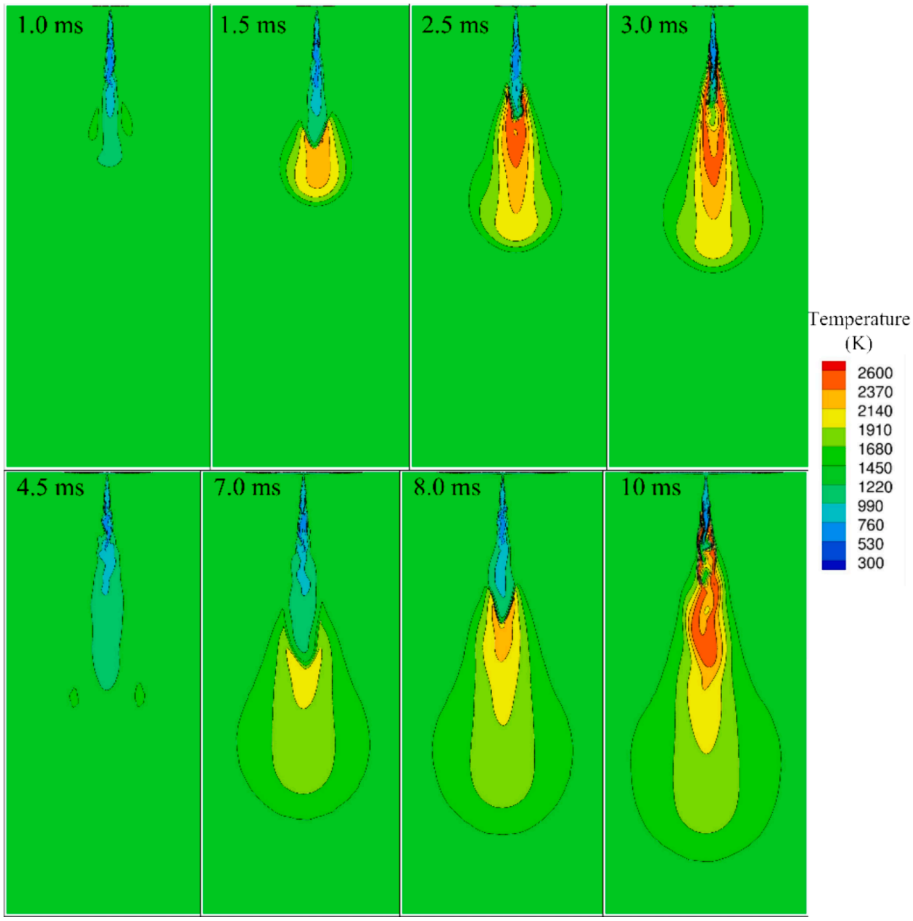

Fig. 15. Comparison between the ignition process by adding 0.085 % mole fraction of hydrogen to the ambient gas (top) and by adding 0.085 % mole fraction of hydrogen as a dissolved gas in the fuel blend. Cases are at 1300 K and 60 bars.

follows: A premixed flame is formed near the injector where the air entrainment occurs creating a premixed mixture. This is followed by a diffusion flame that is further away from the injector. This is a typical structure for a spray flame.

Previously, the facilitation of oxidation and ignition of ammonia spray was achieved by adding trace amount of H_2 to the air in the chamber [17]. By adding hydrogen to the air at elevated conditions, the formation of radicals promoting the oxidation of NH_3 occurs within the spray, due to air entrainment, and at the edge of the spray. Once the fuel evaporates and mixes with the hot products of the exhaust H_2-air mixture, oxidation of NH_3 begins followed by ignition. This case is recreated with the Spray D configuration, including thermodynamic conditions and flow models, to compare the ignition process of each method and provide useful insights into the advantages and drawbacks of each method. Fig. 15 shows a comparison of the ignition process of two cases, one with the addition of H_2 to the air recreated with the Spray D configuration (top) and the case with dissolved hydrogen conducted in this work (bottom). It is evident that a substantial difference is observed in the ignition timing and the flame development speed. The ignition kernels for the dissolved H_2 case begin to form at 4.5 ms while for the H_2 added to the air case begin to form at 1.0 ms. Furthermore, the dissolved H_2 case takes 5.5 ms for the flame to properly develop while adding H_2 to the air results in a flame development duration of 2 ms. For the dissolved H_2 case, there will be a delay in the facilitation of oxidation and ignition of NH_3 as a result of the gaseous H_2 needing to evaporate from the liquid ammonia then mixing with the hot air before igniting. This reiterates the conclusion discussed for Fig. 8 as different concentrations of H_2 result in the same ignition timing. Fig. 16 compares temperature vs mixture fraction for the nonreactive pure ammonia case (top), the H_2 added to the ambient air case (middle), and the 0.085 % H_2 mole fraction dissolved in liquid ammonia (bottom). It can be observed that for every case, there is a sharp drop in temperature for mixture fraction of 0. This is due to the air being cooled near the liquid fuel. Furthermore, due to the lack of ignition in the pure ammonia case, the mixture fraction does not vary at higher temperatures than the 1300 K of the domain. However, the cases where ignition successfully occurs show a peak temperature near the stoichiometric mixture fraction of ammonia with a decline in temperature as mixture fraction increases. Comparison with the successful ignition cases, it is shown that the plots are similar as the addition of hydrogen is in trace amounts. Moreover, the distinction in both cases comes from the ignition timing and the duration for a flame to develop completely as stated before.

In terms of combustion efficiency, both methods show a similar efficiency with a distinction in the flame development speed and ignition timing. However, once ignition occurs both configurations result in the fuel being converted to products, where, using the percentage of NH bond consumption, the dissolved hydrogen case results in a combustion efficiency above 99 %, similar to the H_2 addition from the ambient air case. However, it should be noted that this behavior will most likely be different in engine configurations. Due to the volume of the cylinder when injection occurs, charge-cooling effects, as a consequence of the high latent heat of vaporization of ammonia, will negatively affect the combustion efficiency. Thus, future work is needed in relevant engine configurations to determine the effectiveness of each method.

From this comparison, a trade-off can be observed. H_2 addition to the air requires a more costly change to current engines, whether it is added by on-board thermal cracking or through exhaust gas recirculation. On the other hand, the dissolved H_2 method shows an easier

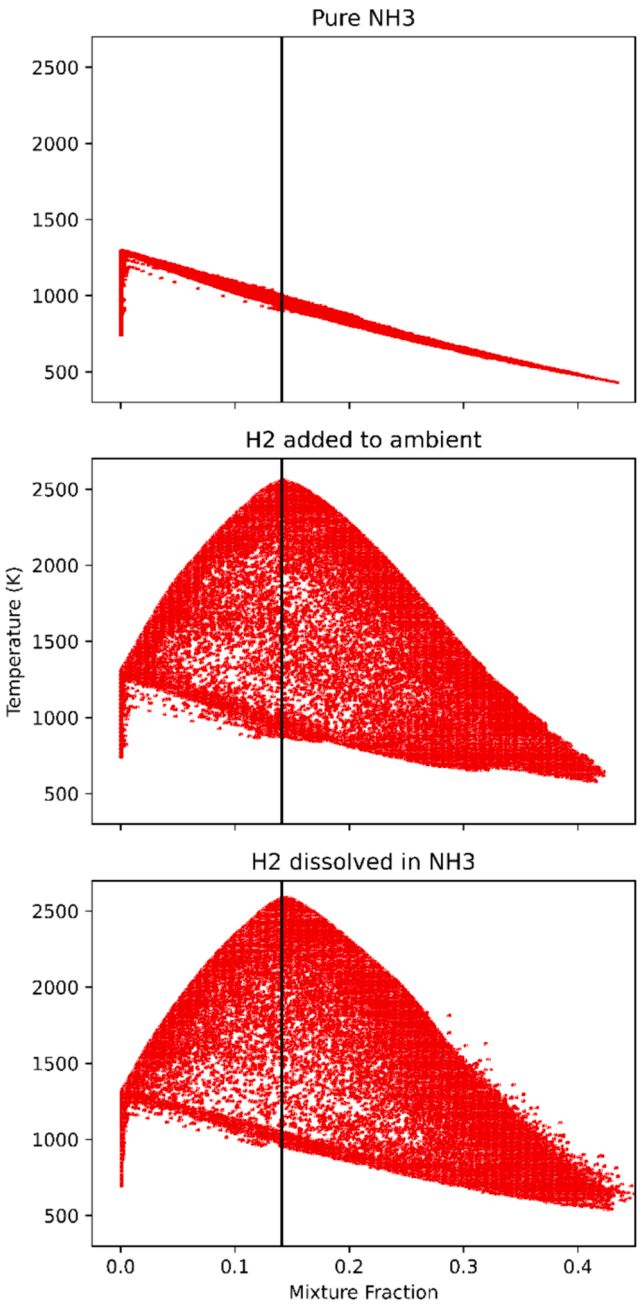

Fig. 16. Temperature vs mixture fraction pure ammonia at the end of injection 4.5 ms, H_2 added to ambient air at the end of injection 4.5 ms, 0.085 % H_2 dissolved in liquid NH_3 at 10.3 ms with an injection duration of 12 ms. The solid line is a reference of stoichiometric mixture fraction, around 0.141.

implementation as the only change needed is for the fuel blend. However, the H_2 addition to the ambient air case demonstrates an improved combustion performance compared to the current work.

3.4. Emissions

Fig. 17 shows the maximum emission mole fractions of the developed flame case with 0.085 % dissolved H_2. The results show the beginning of formation of the emission near 1.5 ms followed by a slight increase before the ignition point. This is attributed to the nitrogen element in the fuel as opposed to traditional hydrocarbons, such as *iso*-octane and n-dodecane, that rely on high temperatures to form emissions from the N_2 in the air. At time of ignition, the NO_x and N_2O are formed in high

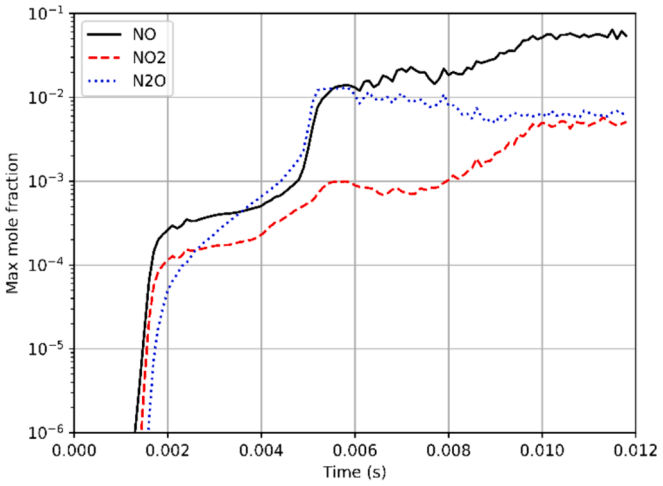

Fig. 17. Evolution of maximum mole fraction of NO, NO_2, and N_2O with time.

concentrations. This increase in emission formation poses a challenge for ammonia as a fuel, specifically N_2O as it has the greenhouse effect 300 times the effect of CO_2. The formation of N_2O matches the trend of NO formation starting with the initial spike observed near 5 ms that then begins to decrease as opposed to NO that continues to increase. On the other hand, NO_2 does not show a sudden increase in concentration, rather a slow gradual increase in concentration. As the flame reaches a quasi-steady state, the emissions begin to stabilize. The largest concentration is attributed to NO having a concentration one magnitude higher than N_2O and NO_2.

Fig. 18 shows the emission mole fraction contour at 10 ms for the developed flame case. As shown, NO concentration is the highest maximum as well as the highest concentration overall in the spray followed by N_2O then NO_2. As the NO is being formed from the fuel and the flame, it continues to propagate. On the other hand, NO_2 and N_2O are shown to be consumed away from the high temperature region. Despite flame development, N_2O remains above 1 ppm away from the flame. However, the maximum concentration is shown near the injector and in the high temperature region. For a better understanding of the underlying kinetics in the formation of NO_x and N_2O, a chemical kinetic pathways diagram is developed. Fig. 19 shows the chemical reaction pathway following the formation of NO_x and N_2O at a high temperature region and low temperature region at 10 ms for the developed case. As shown, the formation of NO near the injector can be traced to the NH, HNO, and HONO intermediates formed, where NH reacts with O_2, HNO reacts with OH and O_2, and HONO reacts with the third body M. The formation of NO is a crucial step in the formation of N_2O and NO_2. The N_2O is mainly formed from NH and N_2H_2 reacting with NO and NO_2 reacting with NH_2. On the other hand, the NO_2 formation is dependent on the reaction of NO with HO_2.

The consumption of these emissions is of interest especially as the burned gas propagates away from the flame. From the fuel, the formation of N_2O is dependent on its reaction with the third body. However, in the flame its consumption is dominant by $N_2O + H \Leftrightarrow N_2 + OH$. The remaining N_2O propagates from the flame to lower temperature regions thus mainly being consumed by $N_2O + M \Leftrightarrow N_2 + O + M$ that is a slow consumption reaction. On the other hand, NO_2 is consumed to form NO from its reaction with OH, M, and H; thus, lower concentrations of NO_2 can be observed. Coupled with the reaction involving HONO and the third body to form more NO, the NO concentration is maintained further away from the flame. Further investigation of emissions is specifically crucial for direct injection application as the local conditions for the fuel mixing and burning are important. It is evident that the formation of these emissions is prevalent within the fuel and controlled thermodynamically, chemically, and by operating conditions such as engine

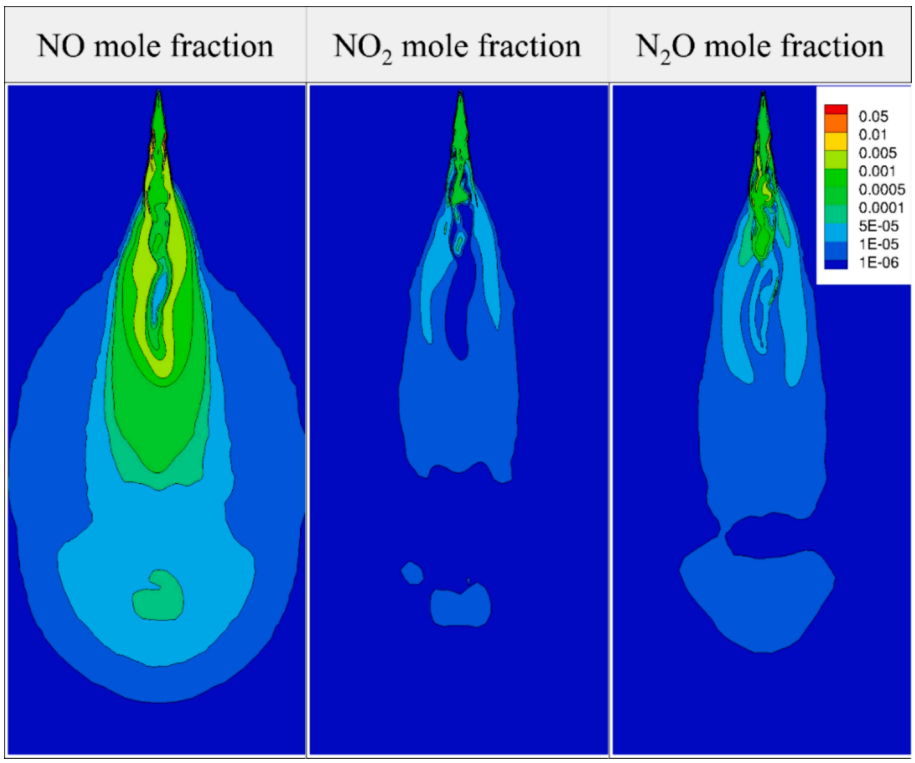

Fig. 18. NO, NO_2, and N_2O mole fraction contours at 10 ms.

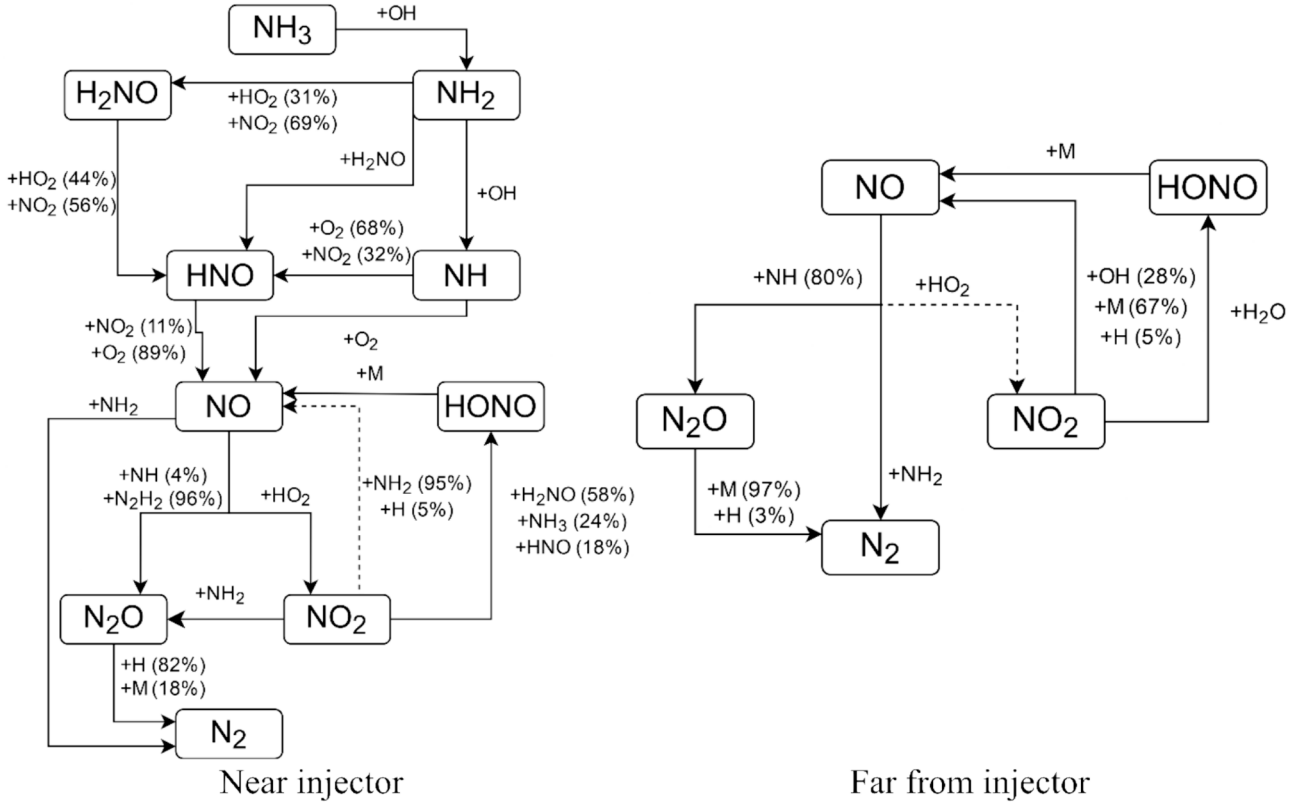

Fig. 19. Reaction pathway following NO_x and N_2O formation at 10 ms near the injector in the high temperature region (left) and away from the injector at a cooler temperature region (right).

speed, initial temperatures, and injection duration. In a direct injection case, the local NO_x and N_2O formation and consumption poses a challenge for NH_3 ignition.

4. Conclusion

This study investigates the facilitation oxidation and ignition of liquid ammonia direct injection using Spray D configuration under engine relevant conditions by the addition of dissolved hydrogen gas in the fuel blend. The results show H_2 addition successfully facilitates ignition of ammonia spray. However, due to the low reactivity of ammonia and high latent heat of vaporization, the flame does not develop completely and is not sustained for an injection duration of 4.5 ms. As such, a complete flame development of ammonia is shown to be made possible with extended injection duration. Furthermore, it is observed that the ignition timing is controlled by the evaporation and mixing of the spray rather than the concentration of H_2. This brings rise to considerations of cost, convenience, and ease for future use of H_2 as a facilitator for NH_3 oxidation and ignition.

The chemical role of hydrogen addition on ignition and emission is examined through the chemical kinetic pathways. It shows the dominant and necessary effects that OH radical from H_2 oxidation plays in oxidizing NH_3 thus generating highly radical intermediates and promoting ignition within desired residence time. Emission results show the high concentrations of NO_x and N_2O before and after the ignition process specifically for NO. The nitrogen element in ammonia coupled with the sensitivity of the emissions to thermodynamic and kinetic effects, results in challenges in controlling emissions globally as they differentiate substantially on the local scale.

In comparison with the previous study on ammonia spray ignition facilitation through the hydrogen addition in the ambient air. By introducing H_2 through the exhaust gas recirculation or on-board thermal cracking, improved combustion characteristics can be achieved, however, more external hardware is needed. On the other hand, the dissolved hydrogen gas and liquid ammonia blend provides a lower cost and convenience advantage. This method tolerates variation in the fuel preparation in terms of hydrogen blending ratio and entails possibly minimal modifications to the injection system.

CRediT authorship contribution statement

Ahmad Hadi Bakir: Writing – original draft, Visualization, Validation, Software, Investigation, Formal analysis. **Haiwen Ge:** Writing – review & editing, Methodology. **Zhili Zhang:** Writing – review & editing, Validation, Project administration, Funding acquisition. **Peng Zhao:** Writing – review & editing, Supervision, Resources, Project administration, Methodology, Funding acquisition, Conceptualization.

Declaration of competing interest

The authors declare that they have no known competing financial interests or personal relationships that could have appeared to influence the work reported in this paper.

Data availability

Data will be made available on request.

Acknowledgment

The authors appreciate the support from NSF through award number 2225803. Convergent Science provided CONVERGE licenses and technical support for this work. Helpful advice from Dr. Lyle Picket from Sandia National Lab and the ECN community is highly appreciated.

References

[1] "Sources of Greenhouse Gas Emissions," [Online]. Available: https://www.epa.gov/ghgemissions/sources-greenhouse-gas-emissions. [Accessed June 2023].
[2] "Report of the Conference of the Parties on its twenty-first session," United Nations, Paris, 2015.
[3] U. S. Geological Survey, "Mineral commodity summaries 2020," U.S. Geological Survey, 2020.
[4] Ghavam S, Vahdati M, Wilson IAG, Styring P. Sustainable ammonia production processes. Front Energy Res 2021;9.
[5] Santhappan JS, Samuel MS, Glivin G, Le T, Mathimani T. Production and utilization of green ammonia for decarbonizing the energy sector with a discrete focus on Sustainable Development Goals and environmental impact and technical hurdles. Fuel 2024;360.
[6] A. Valera-Medina, F. Amer-Hatem, A. K. Azad, I. C. Dedoussi, M. d. Joannon, R. X. Fernandes, P. Glarborg, H. Hashemi, X. He, S. Mashruk, J. McGowan, C. Mounaim-Rouselle, A. Ortiz-Prado, A. Ortiz-Valera, I. Rossetti, B. Shu, M. Yehia, H. Xiao and M. Costa, "Review on Ammonia as a Potential Fuel: From Synthesis to Economics," *Energy & Fuels,* vol. 35, no. 9, pp. 6964-7029, 2021.
[7] "Inventory of U.S. Greenhouse Gas Emissions and Sinks," [Online]. Available: https://www.epa.gov/ghgemissions/inventory-us-greenhouse-gas-emissions-and-sinks. [Accessed December 2023].
[8] Chen J, Jiang X, Qin X, Huang Z. Effect of hydrogen blending on the high temperature auto-ignition of ammonia at elevated pressure. Fuel 2021;287.
[9] S. Wiseman, M. Rieth, A. Gruber, J. R. Dawson and J. H. Chen, "A comparison of the blow-out behavior of turbulent premixed ammonia/hydrogen/nitrogen-air and methane–air flames," *Proceedings of the Combustion Institute,* vol. 38, no. 2, pp. 2869-2876, 2021.
[10] Dinesh MH, Pandey JK, Kumar GN. Study of performance, combustion, and NOx emission behavior of an SI engine fuelled with ammonia/hydrogen blends at various compression ratio. Int J Hydrogen Energy 2022;47(60):25391–403.
[11] A. Bakir, H. Ge and P. Zhao, "Computational Investigation of Combustion Phasing and Emission of Ammonia and Hydrogen Blends under HCCI Conditions," *SAE Technical Paper,* 2023.
[12] Gray JT, Dimitroff E, Meckel NT, Quillian RD. Ammonia fuel - engine compatibility and combustion. SAE Paper 1967;75:785–807.
[13] Nadimi E, Przybyła G, Lewandowski MT, Adamczyk W. Effects of ammonia on combustion, emissions, and performance of the ammonia/diesel dual-fuel compression ignition engine. J Energy Inst 2023;107.
[14] Liu X, Tang Q, Im HG. Enhancing ammonia engine efficiency through pre-chamber combustion and dual-fuel compression ignition techniques. J Clean Prod 2024;436.
[15] Liu Z, Wei H, Shu G, Zhou L. Ammonia-hydrogen engine with reactivity-controlled turbulent jet ignition (RCTJI). Fuel 2023;348.
[16] Huo J, Zhao T, Lin H, Li J, Zhang W, Huang Z, et al. Study on lean combustion of ammonia-hydrogen mixtures in a pre-chamber engine. Fuel 2024;361.
[17] Bakir A, Ge H, Zhang Z, Zhao P. Autoignition enhancement of ammonia spray under engine-relevant conditions via hydrogen addition: Thermal, chemical, and charge cooling effects. Int J Engine Res 2023;24(9):3970–84.
[18] "Spray D Nozzle Geometry," [Online]. Available: https://ecn.sandia.gov/diesel-spray-combustion/target-condition/spray-d-nozzle-geometry/. [Accessed June 2023].
[19] K. J. Richards, P. K. Senecal and E. Pomraning, "CONVERGE 3.1," Convergent Science, Madison, WI, 2023.
[20] Redlich O, Kwong JNS. On the thermodynamics of solutions; an equation of state; fugacities of gaseous solutions. Chem Rev 1949;44(1):233–44.
[21] Launder B, Spalding D. The numerical computation of turbulent flows. Comput Methods Appl Mech Eng 1974;3(2):269–89.
[22] Yakhot V, Smith LM. The renormalization group, the ε-expansion and derivation of turbulence models. J Sci Comput 1992;7:35–61.
[23] R. Reitz and R. Diwakar, "Structure of High-Pressure Fuel Sprays," *SAE Technical Paper,* 1987.
[24] M. A. Patterson, "Modeling the effects of fuel injection characteristics on diesel combustion and emissions [PhD These]," University of Wisconsin-Madison, 1997.
[25] A. A. Amsden, P. J. O'Rourke and T. D. Butler, "KIVA-II: A computer program for chemically reactive flows with sprays," United States, 1989.
[26] Schmidt DP, Rutland C. A new droplet collision algorithm. J Comput Phys 2000;164(1):62–80.
[27] Pelé R, Mounaïm-Rousselle C, Bréquigny P, Hespel C, Bellettre J. First study on ammonia spray characteristics with a current GDI engine injector. Fuels 2021;2:253–71.
[28] Price C, Hamzehloo A, Aleiferis P, Richardson D. An approach to modeling flash-boiling fuel sprays for direct-injection spark-ignition engines. Atom Sprays 2016;26(12):1197–239.
[29] Senecal PK, Pomraning E, Richards KJ. Multidimensional modeling of direct-injection diesel spray liquid length and flame lift-off length using CFD and parallel detailed chemistry. SAE Paper 2003;112:1331–51.
[30] D. G. Goodwin, H. K. Moffat, I. Schoegl, R. L. Speth and B. W. Weber, "Cantera: An object-oriented software toolkit for chemical kinetics, thermodynamics, and transport processes," 2023.
[31] Otomo J, Koshi M, Mitsumori T, Iwasaki H, Yamada K. Chemical kinetic modeling of ammonia oxidation with improved reaction mechanism for ammonia/air and ammonia/hydrogen/air combustion. Int J Hydrogen Energy 2018;43(5):3004–14.
[32] A. Hayakawa, Y. Hirano, E. C. Okafor, H. Yamashita, T. Kudo and H. Kobayashi, "Experimental and numerical study of product gas characteristics of ammonia/air premixed laminar flames stabilized in a stagnation flow," *Proceedings of the Combustion Institute,* vol. 38, no. 2, pp. 2409-2417, 2021.

[33] Maes N, Skeen SA, Bardi M, Fitzgerald RP, Malbec L-M, Bruneaux G, et al. Spray penetration, combustion, and soot formation characteristics of the ECN Spray C and Spray D injectors in multiple combustion facilities. Appl Therm Eng 2020;172:115–36.
[34] Engine Combustion Network, "Request for Experimental and Modeling Contributions," 2012. [Online]. Available: https://ecn.sandia.gov/ecn2-contributions-2/. [Accessed 2024].
[35] Pfohl O, Petkov S, Brunner G. PE 2000: a powerful tool to correlate phase equilibria. Herbert Utz Verlag; 2000.
[36] Markočič E, Knez Ž. Redlich–Kwong equation of state for modelling the solubility of methane in water over a wide range of pressures and temperatures. Fluid Phase Equilib 2016;408:108–14.
[37] Kramberger B, Markocic E, Knez Z. Phase equilibria of binary mixture of carbon monoxide and water at elevated temperatures and pressures. Chem Eng Sci 2013;99:77–80.
[38] Carissimi G, Montalbán MG, Baños FGD, Víllora G. High pressure phase equilibria for binary mixtures of CO2 + 2-pentanol, vinyl butyrate, 2-pentyl butyrate or butyric acid systems. J Supercrit Fluids 2018;135:69–77.
[39] Tagiuri A, Sumon KZ, Henni A. Solubility of carbon dioxide in three [Tf2N] ionic liquids. Fluid Phase Equilib 2014;380:39–47.
[40] Adachi Y, Sugie H. A new mixing rule-modified conventional mixing rule. Fluid Phase Equilib 1986;28.
[41] Wiebe R, Tremearne TH. The solubility of hydrogen in liquid ammonia at 25, 50,75 and 100° and at pressures to 1000 atmospheres. J Am Chem Soc 1934;56(11):2357–60.
[42] Okafor EC, Kurata O, Yamashita H, Inoue T, Tsujimura T, Iki N, et al. Liquid ammonia spray combustion in two-stage micro gas turbine combustors at 0.25 MPa; Relevance of combustion enhancement to flame stability and NOx control. Applic Energy Combust Sci 2021;7.